Formation of Transverse Modes with *Y*-Junction Structures in Broad-Area Oxide-Confined Vertical-Cavity Surface-Emitting Laser

2003 Jpn. J. Appl. Phys. 42 L824

(http://iopscience.iop.org/1347-4065/42/7B/L824)

Jpn. J. Appl. Phys. Vol. 42 (2003) pp. L 824–L 827
Part 2, No. 7B, 15 July 2003

Formation of Transverse Modes with *Y*-Junction Structures in Broad-Area Oxide-Confined Vertical-Cavity Surface-Emitting Laser

Ren-Jay KOU* and Ci-Ling PAN

Institute of Electro-Optical Engineering, National Chiao-Tung University, Hsinchu, Taiwan 300, Republic of China

(Received March 20, 2003; revised manuscript received May 5, 2003; accepted for publication May 14, 2003)

We performed experimental and theoretical investigations on the transverse-mode emission behavior of a broad-area oxide-confined vertical-cavity surface-emitting laser (VCSEL). The far-field emission pattern with y-junction structures is observed in the VCSEL with a 20-μm-diameter aperture when the injection current is significantly above the thermal roll-over point. In order to provide a quantitative understanding of these emission characteristics, we present a numerical simulation to model and fit the experimental results. The numerical simulation adopts the high-order Laguerre-Gaussian mode due to the assumptions of a parabolic refractive-index profile and ring-shaped carrier distribution in the laser. From the numerical simulation results, the formation of *y*-junction structures is inferred to be caused by the superposition of two high-order Laguerre-Gaussian modes. The results of this numerical simulation are in good agreement with the experimental findings. [DOI: 10.1143/JJAP.42.L824]

KEYWORDS: *y*-junction, transverse mode, broad-area oxide-confined vertical-cavity surface-emitting laser, Laguerre-Gaussian mode

Using selective wet oxidation as a means of current constriction and optical confinement has dramatically enhanced the performance of vertical-cavity surface-emitting lasers (VCSELs). As a result record low-threshold currents and high efficiencies have been achieved. In addition to the benefits, the fully three-dimensional extension of the VCSEL cavity together with the transverse device structure introduced by the oxide layer results in numerous new effects which make these VCSELs challenging systems for fundamental physics investigations. One of these aspects is the formation of transverse modes in oxide-confined VCSELs.[1–10] From an applications point of view, this phenomenon gives rise to undesirable effects, such as broadening of the optical spectrum and degradation of the free-space performance due to excessive beam divergence. Therefore, control of the behaviors of transverse modes is a desirable goal, particularly in the numerous applications of broad-area VCSELs such as high-power VCSELs and the application of VCSELs in multimode-fiber data links, as well as for studies of micro cavities, pattern formation in optical systems,[1,9] and dynamics of laser arrays.

In previous studies, the *y*-junction structured pattern can be observed in the interferogram of optical vortices.[11,12] The interference fringe with the *y*-junction structured pattern is called the "edge phase dislocation"[11] or "fork",[12] which is a result of the π-shift in the wave phase located along a line in the transverse plane. In our study, we observe the formation of the *y*-junction structures in very-high-order transverse modes of a broad-area (20 μm in diameter) oxide-confined VCSEL in far-field emission when the injection current is near the thermal turn-off point. For a quantitative interpretation of these characteristics, we adopt the Laguerre-Gaussian ($LG_{p,l}$) mode to model and fit the experimental results, where p and l are the radial and azimuthal indices of the LG mode. The numerical simulation results indicate that the formation of *y*-junction structures is due to the superposition of the high-order LG modes. The numerical results are in excellent quantitative agreement with the experimental observations.

The oxide-confined VCSEL under investigation is grown on a GaAs substrate using metal organic chemical vapor deposition (MOCVD) to operate at a wavelength of approximately 809 nm. The active region consists of three $Al_{0.08}Ga_{0.92}As$-$Al_{0.36}Ga_{0.64}As$ quantum wells, which are embedded in the spacer layers to form a cavity with a thickness of one wavelength. The Bragg mirrors consist of AlGaAs $\lambda/4$ layers with different aluminum contents and graded interfaces in terms of material composition. The confinement of both the carriers and the optical field is achieved by means of a high-Al-content $Al_{0.97}Ga_{0.03}As$ layer in the first top-mirror layer with a central window of unoxidized material. The light output/current (L/I) characteristic of the 20-μm-diameter oxide-confined VCSEL is depicted in Fig. 1, and shows the typical thermal roll-over behavior. Its threshold current is ~2.7 mA and its maximum power is ~6.4 mW. To study the characteristics of its spatial distribution, we couple the near-field images onto the beam profiler using a collimating objective lens. As for far-field images, we project the far-field pattern on a screen and then record it with a CCD camera.

The measured near- and far-field images of the 20-μm-diameter oxide-confined VCSEL are shown in Figs. 2 and 3. The noncircularly symmetric transverse modes can be observed in the near-field images. The oxidized aperture of

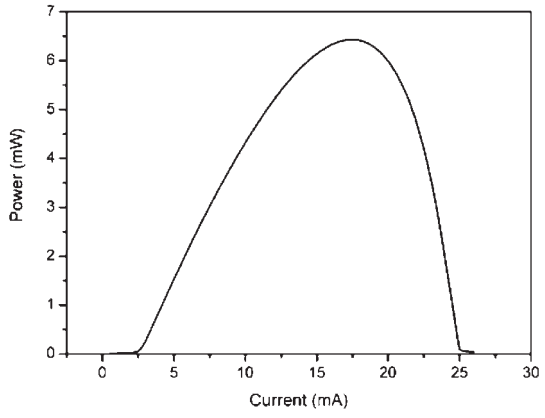

Fig. 1. Output power vs current curve of 20-μm-diameter oxidized VCSEL under CW operation at room temperature.

*E-mail address: rjkou.eo85g@nctu.edu.tw

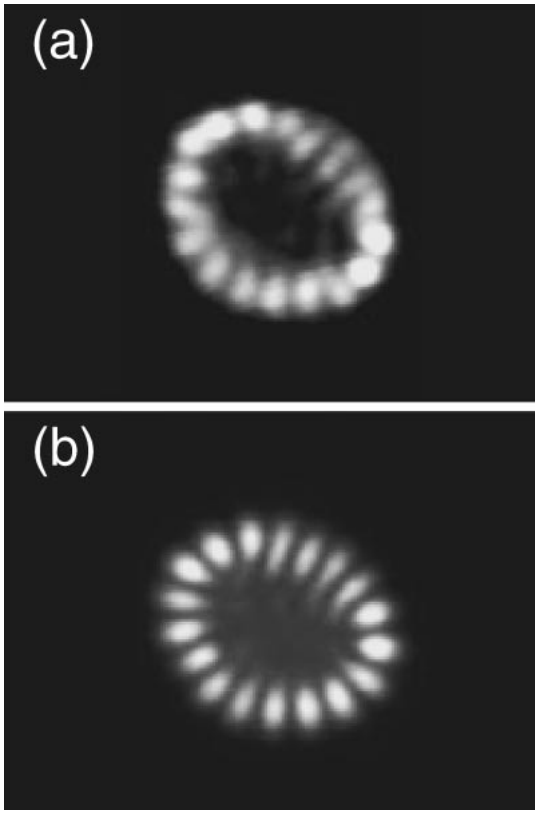

Fig. 2. Experimental near-field patterns of 20-μm-diameter oxidized VCSEL at injection currents of (a) 22.3 mA and (b) 23.3 mA.

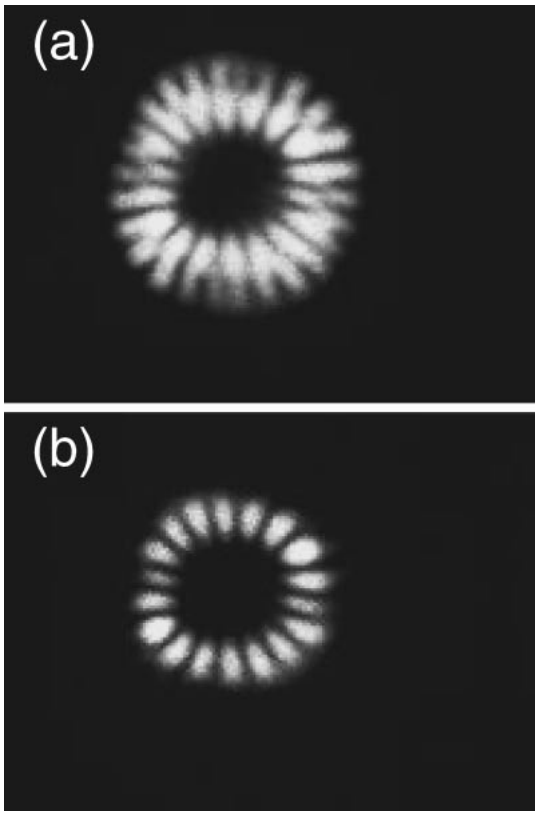

Fig. 3. Experimental far-field patterns of 20-μm-diameter oxidized VCSEL at injection currents of (a) 22.3 mA and (b) 23.3 mA.

our device is not in a circular geometry because of the anisotropic oxidation speed.[7] At 22.3 mA, which corresponds to a negative slope of the *L-I* curve, the high-intensity distribution can only be observed around the periphery of the oxide aperture due to a strong optical confinement provided by oxidized layers. Therefore, the detailed transverse mode structures cannot be resolved in Fig. 2(a). At an even higher injection current of 23.3 mA, the lasing near-field pattern becomes that of a pure single high-order LG mode and exhibits 18 spots, as shown in Fig. 2(b). A pure high-order LG mode has been reported in electrically pumped[3,4] and optically pumped[13] VCSELs. The previous studies suggest that the high-order LG mode is produced by the carrier distribution with a ring-shaped area at the borders of the lasers and a broad minimum in the center. In the far-field image shown in Fig. 3(a), the transverse mode with *y*-junction structures is found at an injection current of 22.3 mA, which is higher than the thermal roll-over point. When the injection current is 23.3 mA, the far-field image turns into that of a 9th-order LG mode, as shown in Fig. 3(b), which is consistent with the near-field image of Fig. 2(b). In particular, the far-field density distributions present a rotation symmetry of π.

We present a numerical simulation for the formation of *y*-junction structures in a broad-area oxide-confined VCSEL, using the high-order LG mode. The guiding of the mode in oxide-confined VCSELs is generally due to a combination of index guiding, thermal index guiding, and carrier-induced index anti guiding. Therefore we assume that the refractive-index profile in the oxide-confined VCSEL is parabolic and that the carriers are distributed in a ring shape at the border of the laser. Based on these assumptions, the preferred laser modes in this case are the $LG_{p,l}$ modes. Each degenerate pair (l) of LG modes gives rise to a pair of daisy modes with $2l$ lobes. The normalized intensity distribution of the LG mode is[13]

$$I(r,\theta,z)=\left[\frac{4}{l!}\frac{1}{w^2(z)}\left(\frac{2r^2}{w^2(z)}\right)^l\exp\left(-\frac{2r^2}{w^2(z)}\right)\right]\left[\frac{1}{\pi}\cos^2(l\theta)\right], \tag{1}$$

with

$$w^2(z)=w_0^2\left[1+\left(\frac{\lambda z}{\pi w_0^2}\right)\right], \tag{2}$$

where $w(z)$ is the Gaussian beam waist parameter, w_0 is the beam waist at $z=0$, and r and θ are the radial and azimuthal coordinates respectively. From the experimental observations, we adopt the $LG_{0,l}$ modes with $l=9$ and $l=13$ to fit the experimental results. Considering the strong optical confinement provided by the oxidized layer, we also assume that the beam waists of the $LG_{0,9}$ and $LG_{0,13}$ modes are similar in the near field. The numerical results of near-field intensity distribution are shown in Fig. 4, which shows the superposition of two high-order LG modes ($LG_{0,9}$ and $LG_{0,13}$ modes) in Fig. 4(a), and the single high-order mode ($LG_{0,9}$ mode) in Fig. 4(b). The result in Fig. 4(b) implies that the $LG_{0,13}$ mode is suppressed due to thermal detuning between the cavity resonance and the quantum well (QW) spectral gain maximum.[6] The corresponding far-field images are presented in Fig. 5. Figure 5(a) shows the calculated result of

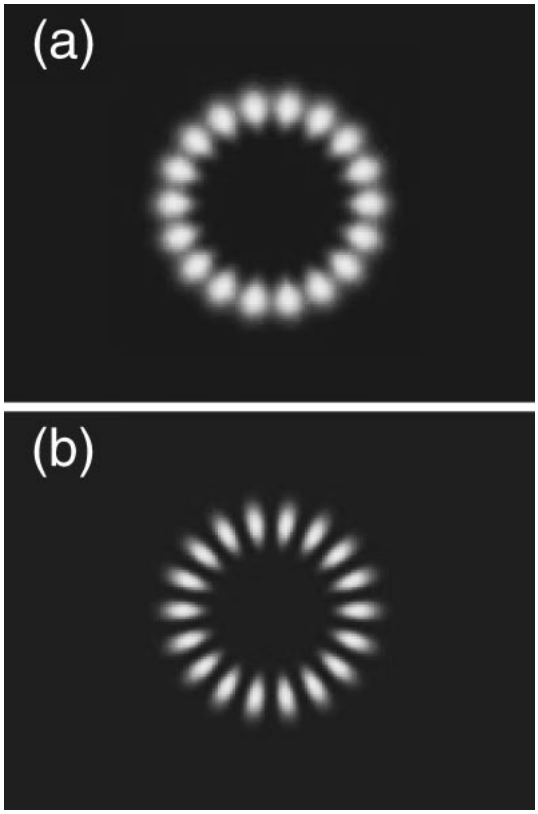

Fig. 4. Computer-calculated near-field patterns corresponding to Fig. 2 for 20-μm-diameter oxidized VCSEL.

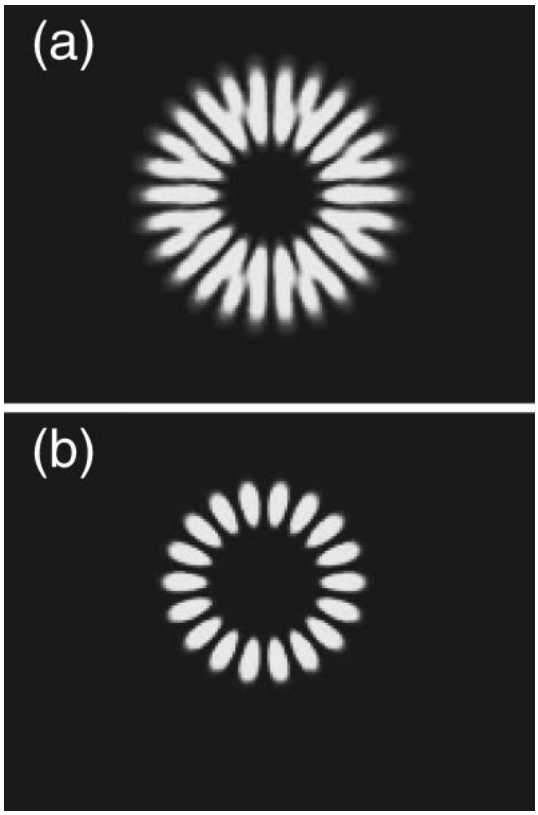

Fig. 5. Computer-calculated far-field patterns corresponding to Fig. 3 for 20-μm-diameter oxidized VCSEL.

the intensity distribution of the superposition of 9th-order and 13th-order LG modes, and Fig. 5(b) shows the intensity distribution of a 9th-order LG mode. In the far field, the beam waist $w(z)$ increases with distance z, then the superposition of two high-order LG modes becomes a different pattern compared to the near-field pattern, as can be seen in Fig. 5(a). This numerical simulation result demonstrates that the formation of *y*-junction structures is induced by the superposition of two high-order LG modes with similar divergent angles.

In previous studies, high-order LG modes usually show up in broad-area VCSELs at high injection currents.[5)] Moreover, the tendency to emit multiple high-order modes in broad-area VCSELs appears to be stronger than in the small-area ones because the inhomogeneous carrier distribution and thermal gradient become more pronounced at the perimeter of larger devices.[5,6,10)] Based on the previous studies and our experimental observations shown in Figs. 2(b) and 3(b), we adopt the high-order LG mode in our simulations under the assumptions of a parabolic refractive-index profile and a ring-shaped carrier distribution.

The ideal VCSEL structure (plano-planar resonator configuration and flat gain; refractive index distribution in the active zone surrounded by an index step due to the oxide aperture) should support linearly polarized modes (LP modes) that are analogous to the ones known from step-index fibers. However, the radial variation of the carrier distribution and the creation of an inhomogeneous temperature profile by ohmic heating will result in some self-focusing in the laser via the dependence of the refractive index on carrier density and temperature. This self-focusing effect can be approximated by a parabolic refractive-index profile. Additionally, strong carrier confinement provided by the oxidized layers, current spreading, and thermal gradient are the dominant factors governing the carrier distribution in the active region of the oxide-confined VCSELs. The combination of these effects causes the carriers to be distributed within a ring-shaped area in the perimeter of the active region. Therefore, a parabolic refractive-index profile and a ring-shaped carrier distribution are reasonable assumptions, and the Laguerre-Gaussian mode is an appropriate eigen function to explain the experimental observations.

According to the experimental and simulation results, the transverse modes with *y*-junction structures can be observed in far-field images at 22.3 mA, which is higher than the thermal roll-over point, and they are formed by two superposed high-order LG modes, $LG_{0,9}$ and $LG_{0,13}$, emitting with similar divergent angles. These multiple high-order modes are confined within the oxide aperture due to the strong optical confinement, so that the details of the transverse modes and the *y*-junction structured pattern cannot be observed in near-field images. At an even higher injection current of 23.3 mA, only $LG_{0,9}$ can be seen because $LG_{0,13}$ is suppressed. The large divergence of $LG_{0,13}$ in the far-field image corresponds to a larger transverse component of the k vector compared to $LG_{0,9}$. The preference for $LG_{0,9}$ is basically determined by the thermal detuning between the cavity resonance and the QW spectral gain maximum. The high-order modes with longer wavelength ($LG_{0,9}$) more efficiency exploit the optical gain, and high-order modes

with shorter wavelength ($LG_{0,13}$) are suppressed at high injection currents. The thermal shift of the emission wavelength at a high injection current is determined by the thermal expansion of the cavity and the thermal increase of the optical index. From the simulation results, we also conclude that the laser supports extremely high-order modes of $LG_{0,9}$ and $LG_{0,13}$. The emission of such high-order modes, even in an electrically pumped VCSEL, can only be possible if the processed wafer is extraordinarily homogeneous.

We presented the results of experimental and numerical investigations of the emission behavior of the 20-μm-diameter oxide-confined VCSEL when the operation current was well above the thermal roll-over point. The near-field images showed that the strong optical confinement introduced by the oxidized layers causes the high-order modes to crowd around the periphery of the oxide aperture so that the *y*-junction structured pattern cannot be observed. The transverse mode with *y*-junction structures could only be observed in far-field images. For the numerical simulation, we assumed a parabolic refractive-index profile and ring-shaped carrier distribution in the laser. Therefore, we adopted the high-order LG modes to model and fit the experimental observations. The formation of the transverse mode with *y*-junction structures is the result of the superposition of $LG_{0,9}$ and $LG_{0,13}$ modes, according to the numerical calculation. We concluded, on the basis of the numerical simulation results, that the inhomogeneous carrier distribution and temperature profile are particularly attractive for building cavities that preferentially operate with multiple high-order modes, leading to the formation of *y*-junction structures. The results of our simulations provide a theoretical explanation of the experimental behavior.

The authors would like to thank Dr. J. S. Pan, H. C. Lai, and M. C. Tang at TrueLight Corp. for their assistance in manufacturing the oxidized VCSEL and Professor K. F. Huang, Assistant Professor Y. F. Chen and Ph. D. student Y. P. Lan at National Chiao-Tung University for the optical measurements and discussions.

1) S. P. Hegarty, G. Huyet, J. G. McInerney and K. D. Choquette: Phys. Rev. Lett. **82** (1999) 1434.
2) H. Deng, Q. Deng and D. G. Deppe: Appl. Phys. Lett. **69** (1996) 3120.
3) Q. Deng, H. Deng and D. G. Deppe: Opt. Lett. **22** (1997) 463.
4) C. Degen, I. Fischer and W. Elsasser: Opt. Exp. **5** (1999) 38.
5) C. Degen, B. Krauskopf, G. Jennemann, I. Fischer and W. Elsasser: J. Opt. B **2** (2000) 517.
6) C. Degen, I. Fischer, W. Elsasser, L. Fratta, P. Debernardi, G. P. Bava, M. Brunner, R. Hovel, M. Moser and K. Gulden: Phys. Rev. A **63** (2001) 023817.
7) P. Debernardi, G. P. Bava, C. Degen, I. Fischer and W. Elsasser: IEEE J. Quantum Electron. **38** (2002) 73.
8) D. L. Huffaker, H. Deng, Q. Deng and D. G. Deppe: Appl. Phys. Lett. **69** (1996) 3477.
9) S. P. Hegarty, G. Huyet, P. Porta, J. G. McInerney, K. D. Choquette, K. M. Geib and H. Q. Hou: J. Opt. Soc. Am. B **16** (1999) 2060.
10) T. Ackemann, S. Barland, M. Cara, S. Balle, J. R. Tredicce, R. Jager, M. Grabherr, M. Miller and K. J. Ebeling: J. Opt. B **2** (2000) 406.
11) D. V. Petrov: Opt. & Quantum Electron. **34** (2002) 759.
12) C. O. Weiss, M. Vaupel, K. Staliunas, G. Slekys and V. B. Taranenko: Appl. Phys. B **68** (1999) 151.
13) S. F. Pereira, M. B. Willemsen, M. P. van Exter and J. P. Woerdman: Appl. Phys. Lett. **73** (1998) 2239.